

## Development of a physical model of saturn's moon enceladus using data from the cassini mission

© A.O. Andreev,<sup>1,2</sup> R.R. Mubarakshina,<sup>1</sup> L.A. Nefediev,<sup>1</sup> Yu.A. Nefedyev,<sup>1</sup> E.A. Chukhlantseva<sup>1</sup>

<sup>1</sup>Kazan Federal University,

420008 Kazan, Russia,

<sup>2</sup>Kazan State Power Engineering University,

420066 Kazan, Russia

e-mail: mubarakshinaregina3@gmail.com, andreev.alexey93@gmail.com

Received May 5, 2025

Revised July 7, 2025

Accepted July 15, 2025

The study addresses the problem of constructing a structural model of Saturn's moon Enceladus. The model was developed based on optical observations from the Cassini–Huygens space mission, employing spherical function expansion and harmonic analysis. Analysis of the 3D model of the moon revealed the presence of three distinct surface types and, when considered alongside other observable geochemical processes, confirmed that this celestial body was formed recently on a cosmic timescale.

**Keywords:** Saturn's moon Enceladus, harmonic modeling, structural analysis.

DOI: 10.61011/TP.2025.12.62491.244-25

Saturn is the sixth planet from the Sun and the second largest in the Solar system, which has the most pronounced external ring. Currently, we know that at least 146 natural Saturn moons exist and among them special scientific interest is paid to Enceladus (Fig. 1), since there are proofs that this moon has geysers [1] that eject water, molecular hydrogen, organic compounds and other substances into space to an altitude of hundreds of kilometers. A specific feature of this Saturn moon is that according to modern gravimetric data there is a liquid water layer of the thickness

of about several kilometers under its surface [2]. A specific composition of the emissions and presence of the liquid water layer make it possible to assume that a lower boundary of the latter has conditions formed, which are suitable for primitive life forms [3]. Morphologically, the Enceladus surface is extremely complex, and based on photographic materials the three most typical types of relief can be identified: a southern subpolar regions exhibit deep cracks extending for more than one hundred kilometers, and there are also old regions with traces of multiple impact events, and the third type of the surface is portions that are characterized by a low crateral degree and probably smoothed due to high intensity of internal geological processes. Traditionally, this division is related to tide effects by a central body on the moon. The present study has investigated data of Enceladus optical observations (EOO), which were obtained by the Cassini–Huygens mission [4], thereby making it possible to create an Enceladus structure model.

Twelve observation tools of the Cassini orbiter were used for performing a complex scientific experiment. For the period of its mission, the Cassini orbiter made a number of approachings with Enceladus for the period 2004–2017. At the same time, diverse data types were obtained, including radiometric and optical observations. The former were further applied for studying a gravitational field, so were the latter for investigating the moon surface and determining parameters of its revolution [5]. Optical images were obtained by means of a monochromatic narrow-angle camera (NAC) and a wide-angle camera (WAC) with a pixel surface scale from 3 to 14 km. We used the Enceladus topography obtained in the study [5] and stereophotoclinometrically summarized into a unified system by iterations. The further stages of altimetry investigation included the following. As

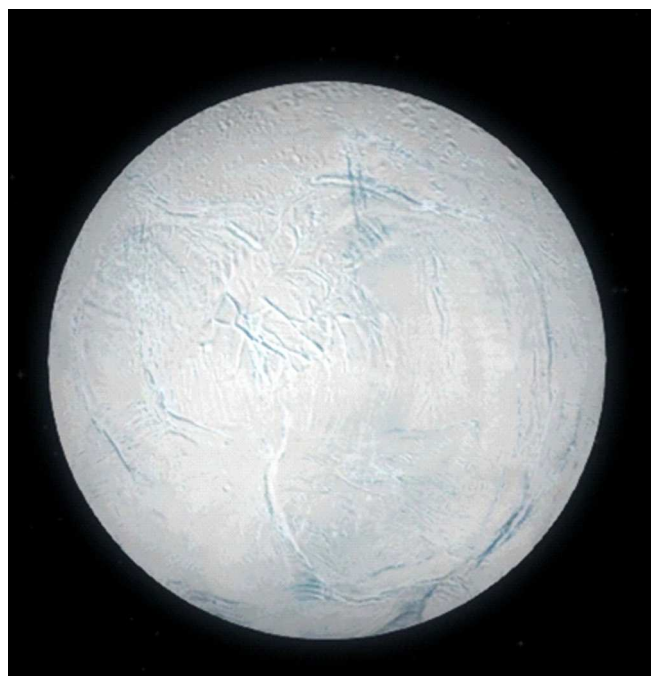


**Figure 1.** Satellite image of the Saturn's moon Enceladus.

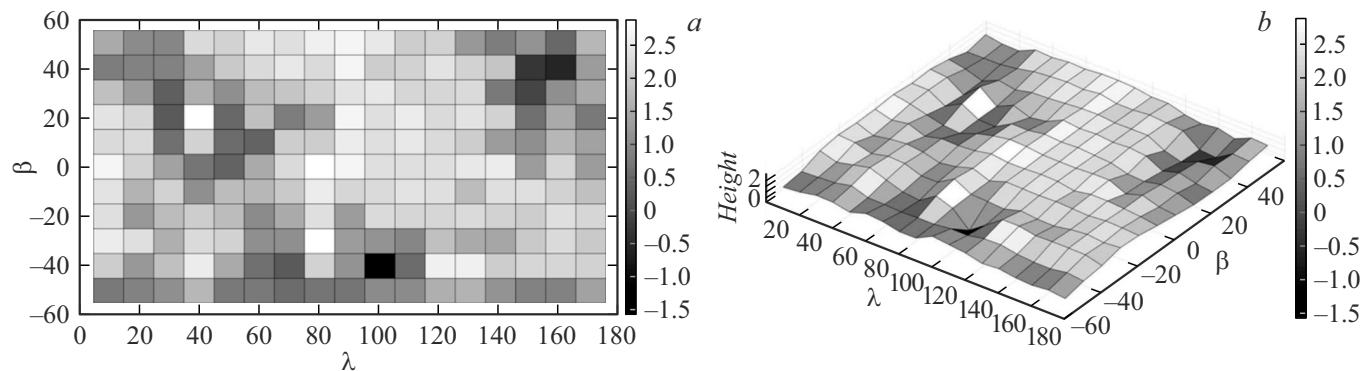


**Figure 2.** Relief of the Enceladus surface with altitude averaging with a step  $10 \times 10^\circ$  in the 2D- and 3D-formats from  $0^\circ$  to  $180^\circ$  along the longitude and from  $60^\circ$  to  $-60^\circ$  along the latitude.

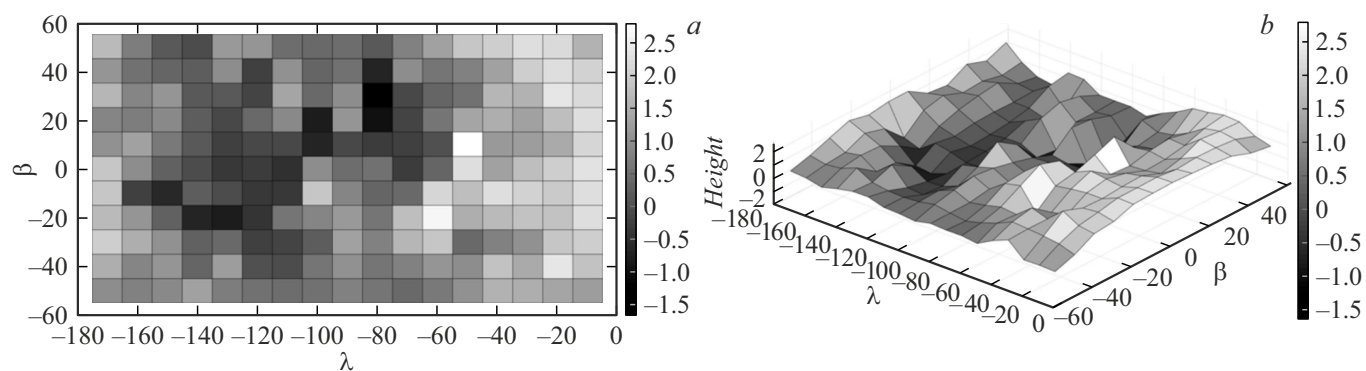


**Figure 3.** Relief of the Enceladus surface with altitude averaging with a step  $10 \times 10^\circ$  in the 2D- and 3D-formats from  $-180^\circ$  to  $0^\circ$  along the longitude and from  $60^\circ$  to  $-60^\circ$  along the latitude.

a model that describes the topographic specific features of Enceladus, an altimetry function was represented as a series of spherical functions in a regression form [6]:

$$h(\lambda, \beta) = \sum_{n=0}^N \sum_{m=0}^n \left( \bar{C}_{nm} \cos m\lambda + \bar{S}_{nm} \right) \sin m\lambda \cdot \bar{P}_{nm}(\cos \beta) + \varepsilon, \quad (1)$$

where  $\lambda, \beta$  are spherical selenographic coordinates the longitude and the latitude;  $C_{ik}, S_{ik}$  are normalized harmonic amplitudes;  $P_{ik}$  are Legendre functions;  $\varepsilon$  is a random regression error.

The system (1) is solved for the Enceladus macrofigure model by means of regression modeling. When estimating the coefficients  $C_{ik}, S_{ik}$ , robust statistical indices were used. When the data were reduced, fulfillment of the main conditions of the least-square method was monitored and adaptation procedures were performed in case of their violation. The methods of Householder and Gauss-Jordan were used a basic mathematical approach. As a result, the Enceladus macromodel was constructed using the SURFER software package.

Fig. 2 and 3 shows two-dimensional and three-dimensional diagrams, which demonstrate average values of the altitudes for the regions of the size  $10^\circ \times 10^\circ$ .

The 3D-surface model was structurally analyzed from  $0^\circ$  to  $180^\circ$  in the longitude and from  $60^\circ$  to  $-60^\circ$  in the latitude to select an altitude maximum and an altitude minimum:  $H_{\max} = 2.88$  km (coordinates of a point by the selenographic latitude and longitude:  $\beta = -30^\circ, \lambda = 80^\circ$ ) and  $H_{\min} = -1.58$  km (coordinates of a point by the selenographic latitude and longitude:  $\beta = -40^\circ, \lambda = 100^\circ$ ).

The 3D-model of the Enceladus surface was structurally analyzed (Fig. 3) from  $-180^\circ$  to  $0^\circ$  in the longitude and from  $60^\circ$  to  $-60^\circ$  in the latitude to select a maximum and a minimum in the altitude in km  $H_{\max} = 2.7900$  (coordinates of a point by the selenographic latitude and longitude:  $\beta = 10^\circ, \lambda = -50^\circ$ ) and  $H_{\min} = -1.69$  (coordinates of a point by the selenographic latitude and longitude:  $\beta = -40^\circ, \lambda = 80^\circ$ ).

Fig. 4 shows the 3D-model of the Saturn moon, which is created using a software algorithm based on expansion of the altimetry data of satellite observations by spherical functions.

It can be seen after analyzing the 3D-model of the Saturn's moon Enceladus (Fig. 4) that the regions from  $0^\circ$  to  $40^\circ$  and from  $-60^\circ$  to  $0^\circ$  in the longitude and the latitude, respectively, as well as from  $0^\circ$  to  $80^\circ$  and from  $20^\circ$  to  $60^\circ$  and from  $140^\circ$  to  $180^\circ$  and from  $-60^\circ$  to  $0^\circ$  exhibit

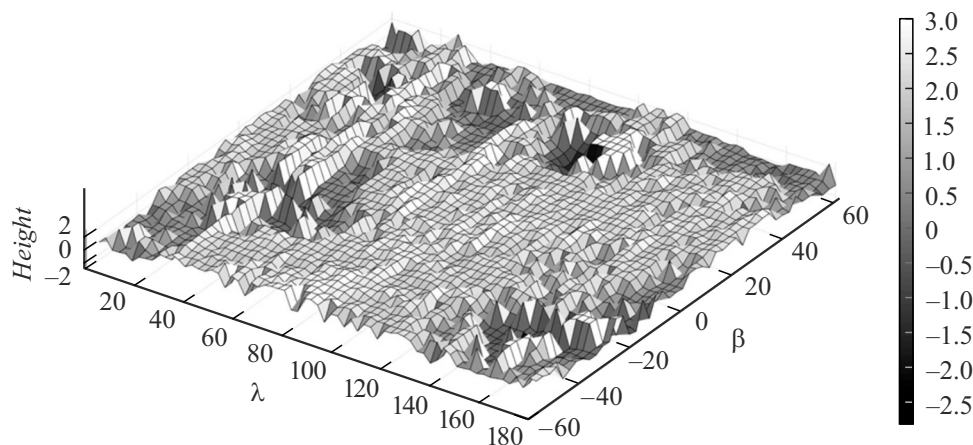


**Figure 4.** 3D-model of the Saturn's moon Enceladus.

an uneven mountain structure of terrain, while a placid and even relief is common in the other regions.

It should be noted that the 3D-models shown in Fig. 2–4 differ by a detail degree and the Figures 2 and 4 cover another surface range unlike Fig. 3.

Based on results of investigation of the diagrams provided herein, one can recommend an area that is the most favorable for landing to the Saturn's mood and stretches from  $15^\circ$  to  $25^\circ$  in the latitude and from  $-115^\circ$  to  $125^\circ$  in the longitude. A spacecraft can also be safely landed within an area between the latitudes from  $-30^\circ$  to  $-55^\circ$  and the longitudes from  $-148^\circ$  to  $155^\circ$ .

Summarizing, it should be noted that:

1) Enceladus is the magnitude-sixth natural moon of Saturn and is very similar to Titan in the size. It should be reminded that Titan is the largest moon of Saturn which has an atmosphere and the only body in the Solar system (except for the Earth), which contains a liquid component. Furthermore, Enceladus has the largest reflective surface among all the celestial bodies of the Solar system and, therefore, it is slightly heated under effect of solar radiation. The moon surface has a diverse structure: crater areas, mountain-like massives and relief-smoothened zones;

2) geological experiments directly on the Enceladus surface require a more advanced level of scientific equipment, and the leading space agencies do not plan such studies at the moment;

3) based on the obtained results, it can be noted that Enceladus relief variations as well as a distribution of topographic specific features associated with the impact events confirm a hypothesis of its quite young period of formation.

Based on results of investigation, the Enceladus surface can be divided into three categories: the regions including impact craters (which follows from analysis of the satellite images in Fig. 1), the uneven-relief zones and the least-uneven portions. The obtained results confirm complexity of the moon surface: large height

differences and faults can indicate quite recent formation of some relief forms and evolutional renewal of the surface.

The 3D-model of Enceladus will be used for studying astrophysical parameters [7,8] and a structure of the moon when engineering Enceladus missions and for building theories of evolution of the Saturn system and the Solar system as a whole.

## Funding

This work/publication was funded by a grant from the Academy of Sciences of the Republic of Tatarstan provided to higher education institutions, scientific and other organizations to support human resource development plans in terms of encouraging their research and academic staff to defend doctoral dissertations and conduct research activities (Agreement No. 12/2025-PD-KFU dated December 22, 2025).

## Conflict of interest

The authors declare that they have no conflict of interest.

## References

- [1] C.C. Porco, P. Helfenstein, C. Thomas, A.P. Ingersoll, J. Wisdom, R. West, G. Neukum, T. Denk, R. Wagner, T. Roatsch, S. Kieffer, E. Turtle, A. McEwen, T.V. Johnson, Rathbun, J. Veverka, D. Wilson, J. Perry, J. Spitale, A. Brahic, J.A. Burns, A.D. DelGenio, L. Dones, C.D. Murray, S. Squyres. *Science*, **311** (5766), 1393 (2006). DOI: 10.1126/science.1123013
- [2] S. Iess, D.J. Stevenson, M. Parisi, D. Hemingway, R.A. Jacobson, J.I. Lunine, F. Nimmo, J.W. Armstrong, S.W. Asmar, M. Ducci, P. Tortora. *Science*, **344** (6179), 78 (2014) DOI: 10.1126/science.1250551
- [3] J.H. Waite, C.R. Glein, R.S. Perryman, B.D. Teolis, B.A. Magee, G. Miller, J. Grimes, M.E. Perry, K.E. Miller, A. Bouquet, J.I. Lunine, T. Brockwell, S.J. Bolton. *Science*, **356** (6334), 155 (2017). DOI: 10.1126/science.aa18703

- [4] D.L. Matson, L.J. Spilker, J.P. Lebreton. *Space Sci. Rev.*, **104** (1–4), 1 (2002). DOI: 10.1023/a:1023609211620
- [5] R.S. Park, N. Mastrodemos, R.A. Jacobson, A. Berne, A.T. Vaughan, D.J. Hemingway, E.J. Leonard, J.C. Castillo-Rogez, C.S. Cockell, J.T. Keane, A.S. Konopliv, F. Nimmo, J.E. Riedel, M. Simons, S. Vance. *J. Geophys. Research: Planets*, **129** (1), e2023JE008054 (2024).  
<https://doi.org/10.1029/2023JE008054>
- [6] A.O. Andreev, Yu.A. Nefedyev, N.Yu. Demina, L.A. Nefediev, N.K. Petrova, A.A. Zagidullin. *Astronom. Reports*, **64** (9), 795 (2020). <https://doi.org/10.1134/S1063772920100017>
- [7] A.O. Andreev, E.N. Akhmedshina, L.A. Nefediev, Yu.A. Nefedyev, N.Yu. Demina. *Astronomy Reports*, **65** (5), 435 (2021). DOI: 10.1134/S1063772921060019
- [8] M.V. Sergienko, M.G. Sokolova, Y.A. Nefedyev, A.O. Andreev. *Astron. Rep.*, **64**, 1087 (2020).  
DOI: 10.1134/S1063772920120124

*Translated by M.Shevlev*